



## Electrospinning of the laser dye rhodamine B-doped poly(methyl methacrylate) nanofibers

RAMDAN M. DUKALI<sup>1</sup>, IVANA M. RADOVIĆ<sup>1</sup>, DUŠICA B. STOJANOVIĆ<sup>1</sup>,  
DRAGUTIN M. ŠEVIĆ<sup>2</sup>, VESNA J. RADOJEVIĆ<sup>1\*</sup>, DRAGAN M. JOCIĆ<sup>1</sup>  
and RADOSLAV R. ALEKSIĆ<sup>1</sup>

<sup>1</sup>University of Belgrade, Faculty of Technology and Metallurgy, Belgrade and <sup>2</sup>University of Belgrade, Institute of Physics, Belgrade, Serbia

(Received 24 October 2013, revised 27 January, accepted 30 January 2014)

**Abstract:** The electrospinning of rhodamine B (RhB)-doped poly(methyl methacrylate) (PMMA) is presented as a promising technique for processing photoluminescent nanofibers. Nanofibers with concentrations of RhB in PMMA between 0.05 and 2.0 wt. % were studied. The FTIR spectrum, fiber morphology, thermal properties and optical properties of the nanofibers were investigated. Smooth, bead-free and nonporous nanofibers were obtained. Differential scanning calorimetry (DSC) results revealed that the glass transition temperature of the PMMA ( $T_g$ ) increased with the increasing of RhB content up to 0.5 wt. % and thereafter decreased. The laser induced fluorescence (LIF) technique was used to study the fluorescence properties of the nanofibers. The maximum fluorescence emission was observed at a concentration of RhB of 0.2 wt. %.

**Keywords:** electrospinning; nanofibers; dye-doped PMMA; fluorescence.

### INTRODUCTION

Polymer nanofibers offer a great opportunity for applications beyond nanoelectronics,<sup>1,2</sup> such as, for membrane materials,<sup>3</sup> tissue scaffolding and other biomedical applications,<sup>4</sup> sensing<sup>5</sup> and as reinforcements in composite materials.<sup>6,7</sup> Moreover, the properties of these nanoscale polymeric structures make them interesting candidates for the next generation of photonic devices.<sup>8,9</sup> For example, fibrous dielectric nanostructures could be used as single-mode light waveguides,<sup>10</sup> sensors<sup>5</sup> or building blocks of photonic band-gap materials.<sup>11</sup> Polymer nanofibers could be fabricated by diverse methods, including polymerization in nanoporous templates<sup>12</sup> dip-pen lithography<sup>13</sup> self-assembly,<sup>14</sup> direct drawing from polymer solutions<sup>15</sup> and molding,<sup>16</sup> although only electrospin-

\*Corresponding author. E-mail: vesnar@tmf.bg.ac.rs  
doi: 10.2298/JSC131014011D

ning<sup>17–22</sup> assures a low cost and high throughput production. Electrospinning is a versatile technique that has recently undergone significant development in the production of nanofibers. The polymer fibers are formed from a solution between two electrodes bearing electrical charges of opposite polarity. One of the electrodes is placed into the solution and the other onto a collector. Once ejected out of a metal needle, the charged solution of the jets evaporates to become fibers, which are collected on the collector. The structure and the morphology of electrospun polymer materials, be it fibers or particles, are determined by the synergistic effects of solution parameters (polymer concentration, solution viscosity and flow rate) and electrostatic forces (applied voltage and distance between the needle and collector).

A major advantage of electrospinning is the possibility to produce hybrid, functional photonic materials by incorporating, *e.g.*, light emitters into the fibers.<sup>23–25</sup> The polymer, the light emitter and the characteristic dimension (diameter of the fibers) can be varied independently, therefore allowing for a wide range of applications. Both organic dye molecules and inorganic materials can be embedded into the fibers. Organic dye-doped polymers have been widely investigated as gain media in solid-state dye lasers.<sup>26–29</sup> Dye molecules, which have large absorption and induced emission cross sections due to allowed  $\pi$ – $\pi$  transitions, are ideal active dopants for the generation and amplification of intense light pulses. Thus, many research groups have synthesized and tested numerous chemical substances that were proved good laser dyes. The dye has, however, to be embedded in a suitable matrix or host. The incorporation of a dye in liquid media adversely affects many thermodynamic and spectroscopic properties of the dye (kinetics of energy up-conversion). The adding of dye in polymer solution changes the viscosity of the solution and hence, influences the process of electrospinning.

Thermoplastic PMMA is considered as one of the most efficient dye matrices with excellent optical, thermal, photochemical and dimensional stability. As such, it has been widely used for laser and non-linear optical materials. The incorporation of rhodamine B (RhB) in the host polymer would obviously induce structural and morphological changes.<sup>30,31</sup>

Critical factors determining the optical response of dyes are related to the extent to which their physical and chemical properties are maintained. Thermal and optical properties of dye-doped polymers are important for the identification of suitable laser media. RhB is of great interest as it processes the highest photostability,  $\approx 9,000$  GJ mol<sup>-1</sup>.<sup>32</sup>

In this work, the electrospinning of PMMA–RhB nanofibers was performed, and the structure, morphology, and the linear and nonlinear optical properties of the resulting fibers were investigated.

## EXPERIMENTAL

Commercially available PMMA Acryrex® CM205 (Chi Mei Corp.) ( $\bar{M}_w \approx 90400 \text{ g mol}^{-1}$ ) pellets were used as the matrix for preparing the samples. Dimethylformamide (DMF, anhydrous, 99.8 %, Sigma–Aldrich) was chosen as the solvent and the laser dye RhB (Sigma–Aldrich,  $M = 479.01 \text{ g mol}^{-1}$ ) was chosen for incorporation into the polymer matrix. The aim of starting experiments was to establish the conditions for PMMA fiber electrospinning. Homogenous solutions of the polymer were obtained by magnetically stirring for 48 h at room temperature. The concentrations of PMMA in the DMF solutions were 6 and 22 wt. %, according to literature data.<sup>24</sup> The electrospinning was performed on an Electrospinner CH-01, Linari Engineering, Italy. A plastic syringe (20 mL) with a metallic needle of 1 mm inner diameter was set vertically on the syringe pump (R-100E, RAZEL Scientific Instruments) and the high-voltage power supply (Spellman High Voltage Electronics Corporation, model: PCM50P120) was set to a voltage of 28 kV. The distance of the needle tip from the collector was 15 cm and different flow rates were employed (5, 1 and 0.5 mL h<sup>-1</sup>). Electrospun fibers were dried for 8 h at 50 °C in a vacuum drying oven. The morphology of nanofibers was obtained using a field emission scanning electron microscope (FESEM, TESCAN MIRA 3) with the fracture surfaces sputtered with gold. SEM analysis revealed that the best results were achieved with a 22 wt. % solution of PMMA in DMF at a flow rate of 0.5 mL h<sup>-1</sup>. For this reason, it was decided to use this set of parameters for the fabrication of RhB-doped PMMA fibers.

The procedure for preparing the solutions for the production of RhB-doped PMMA fibers was similar to that employed for the fabrication of pure PMMA fibers. Homogenous solutions of polymer were obtained by magnetically stirring for 48 h at room temperature and after dissolution of the polymer, the dye was directly added into the solution and the stirring was continued for a further 10 min. The contents of RhB in the PMMA were 0.05, 0.1, 0.2, 0.5, 1.0 and 2.0 wt. % after evaporation of the solvent. The rheological behavior of the PMMA dye solutions was analyzed using a Discovery hybrid rheometer HR2 (TA instruments) with parallel plate (diameter 25 mm; gap 500 µm) geometry at 25 °C. The flow characteristics (steady-shear measurements) of the samples were measured by varying the shear rate from 1 to 2000 s<sup>-1</sup>.

The electrospinning process was setup as in the previously performed experiments: the applied voltage was 28 kV, the flow rate of polymer solution was constant at 0.5 ml h<sup>-1</sup> and the distance of the needle tip from the collector was 15 cm. All samples were obtained at 20 °C and 30 % air humidity. The obtained nanofibers were dried in a vacuum oven for 20 h at 80 °C.

The infrared (IR) spectra of samples in KBr discs were obtained by transmission Fourier transform infrared (FTIR) spectroscopy (Hartmann & Braun, MB-series). The FTIR spectra were recorded between 4000 and 400 cm<sup>-1</sup> with a resolution of 4 cm<sup>-1</sup>.

The diameter of the electrospun nanofibers was measured by Image Pro Plus 4.0 (100 measurements per photo). Differential scanning calorimetry (DSC) measurements were conducted using a TA Instruments, TA DSC Q10 instrument calibrated with indium standards. The samples mass was 0.5 mg. The measurements were performed under a dynamic nitrogen flow of 50 mL min<sup>-1</sup> in the temperature range from 30 to 155 °C. The samples were heated up to 155 °C at a rate of 10 °C min<sup>-1</sup>, kept at 155 °C for 5 min to erase thermal history and then cooled to 30 °C at the same rate. A second heating was performed on each sample. The glass transition temperature was determined at the midpoint of the initial slope change.

The basic setup of the time-resolved laser-induced fluorescence measurement system consisted of an Nd–YAG Vibrant OPO laser system and a Hamamatsu streak camera. The

output of the OPO could be continuously tuned over a spectral range from 320 to 475 nm. After analysis of the preliminary results, for measurements presented herein, the second harmonic of the Nd-YAG laser, 532 nm, was used as an excitation source of the samples. The wavelength of 532 nm is closer to the absorption peak of RhB than the OPO output. The emission spectra were recorded using a streak scope (Hamamatsu model C4334-01) with an integrated video streak camera. The fluorescence emission was collected at 90° to the excitation and dispersed by a 0.3 m focal length triple grating imaging spectrograph (SpectraPro-2300i). A grating of 50 g mm<sup>-1</sup> was used to cover the 330 nm spectral range.

## RESULTS AND DISCUSSIONS

In the initial experiments of electrospinning the PMMA solutions, nanofibers with three kinds of morphologies were obtained, *i.e.*, ring-like particles, bead-like

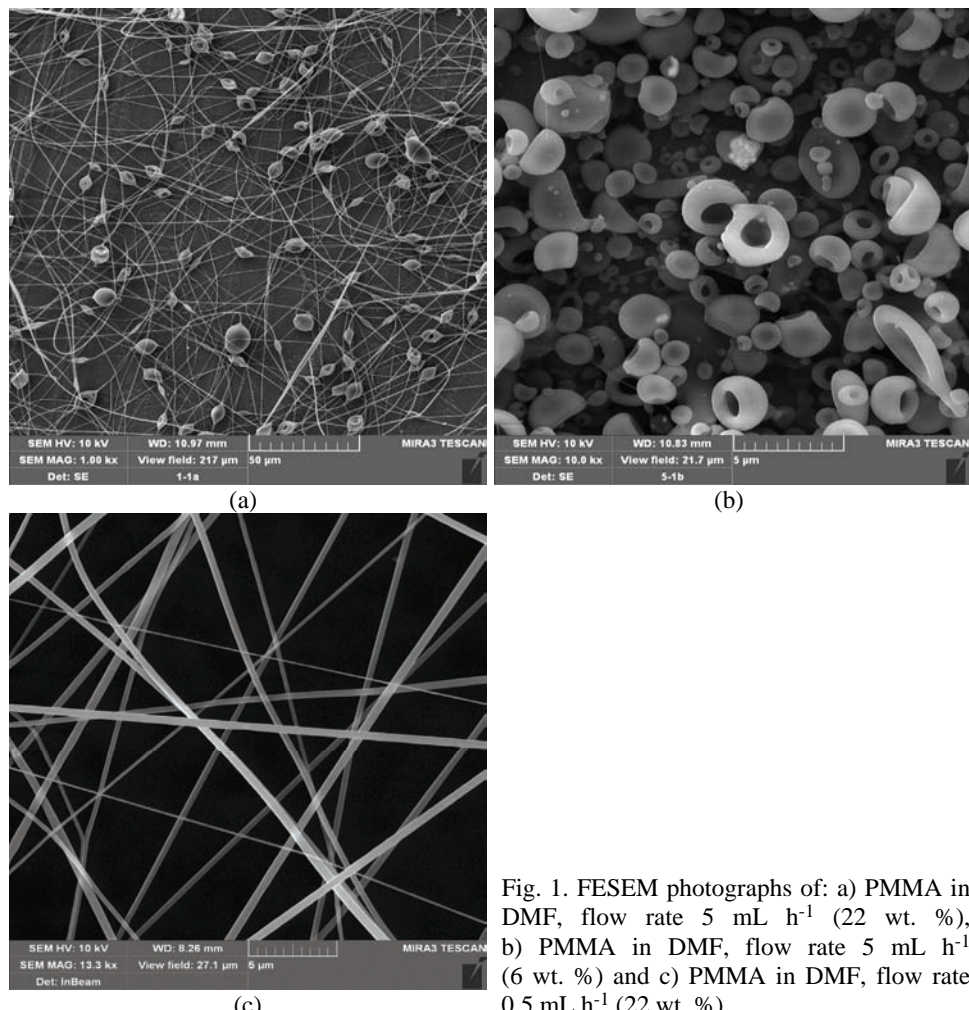


Fig. 1. FESEM photographs of: a) PMMA in DMF, flow rate 5 mL h<sup>-1</sup> (22 wt. %), b) PMMA in DMF, flow rate 5 mL h<sup>-1</sup> (6 wt. %) and c) PMMA in DMF, flow rate 0.5 mL h<sup>-1</sup> (22 wt. %).

nanofibers and ultrafine nanofibers. As shown in Fig. 1a, bead-like nanofibers were fabricated from the 22 wt. % PMMA in DMF solution at a flow rate of 5 mL h<sup>-1</sup>. The ring-like morphology (Fig. 1b) was obtained from the 6 wt. % PMMA in DMF at a flow rate of 1 mL h<sup>-1</sup>. Electrospinning at relatively low polymer concentrations resulted in particles rather than fibers.<sup>33</sup> It is obvious that the jet of polymer solution from the tip of the capillary began to break up into droplets at the lower polymer concentration. The solution viscosity should be above a minimum for fiber formation, *i.e.*, if the viscosity was too low, the process resulted in electrospraying to yield vesicles under the influence of an electric field. Smooth, bead-free nanofibers were produced with a combination of higher concentration and lower rate (22 wt. % solution of PMMA in DMF at a flow rate of 0.5 mL h<sup>-1</sup>). For this reason, it was decided to use this set of parameters to continue with the experiments in which PMMA fibers doped with RhB were fabricated.

The viscosities of solutions (measurements at shear rate 100 s<sup>-1</sup>) containing various concentrations of RhB are listed in Table I. FESEM photographs of the PMMA–RhB nanofibers are presented in Fig. 2a. Image analysis revealed that the nanofibers were beads-free and with a smooth surface. These fibers presented regular surface morphologies.

TABLE I. Viscosity of solutions and diameter of electrospun nanofibers from image analysis

Concentration of RhB, wt. %	Viscosity, Pa s	Mean diameter of fibers, nm
0	2.23	1395±262
0.05	1.75	1068±306
0.1	1.72	967±258
0.2	1.80	650±90
0.5	1.90	743±98
1.0	1.72	598±115
2.0	1.82	623±112

During the electrospinning process, a polymer solution is drawn from the nozzle of the spinneret and the electrical properties, viscosity and surface tension of the solution determine the extent of stretching of the solution under electrostatic forces. The smaller diameter of the nanofibers from the lower viscosity solution is the result of the solution being stretched easily during electrospinning. The larger nanofiber diameters are attributed to the viscosity of the solution being high enough to lower the bending instability of the jet. The solution becomes resistant to stretching by the electrical charges on the electrospinning jet. From Table I, it is obvious that the fiber diameter decreased as the viscosity of solution decreased from that of pure PMMA to that of the 0.05 wt. % RhB doped PMMA. Subsequently, the value the change in viscosity was in the range of 10 %, but the diameter of the nanofibers continually decreased. The explanation for such beha-

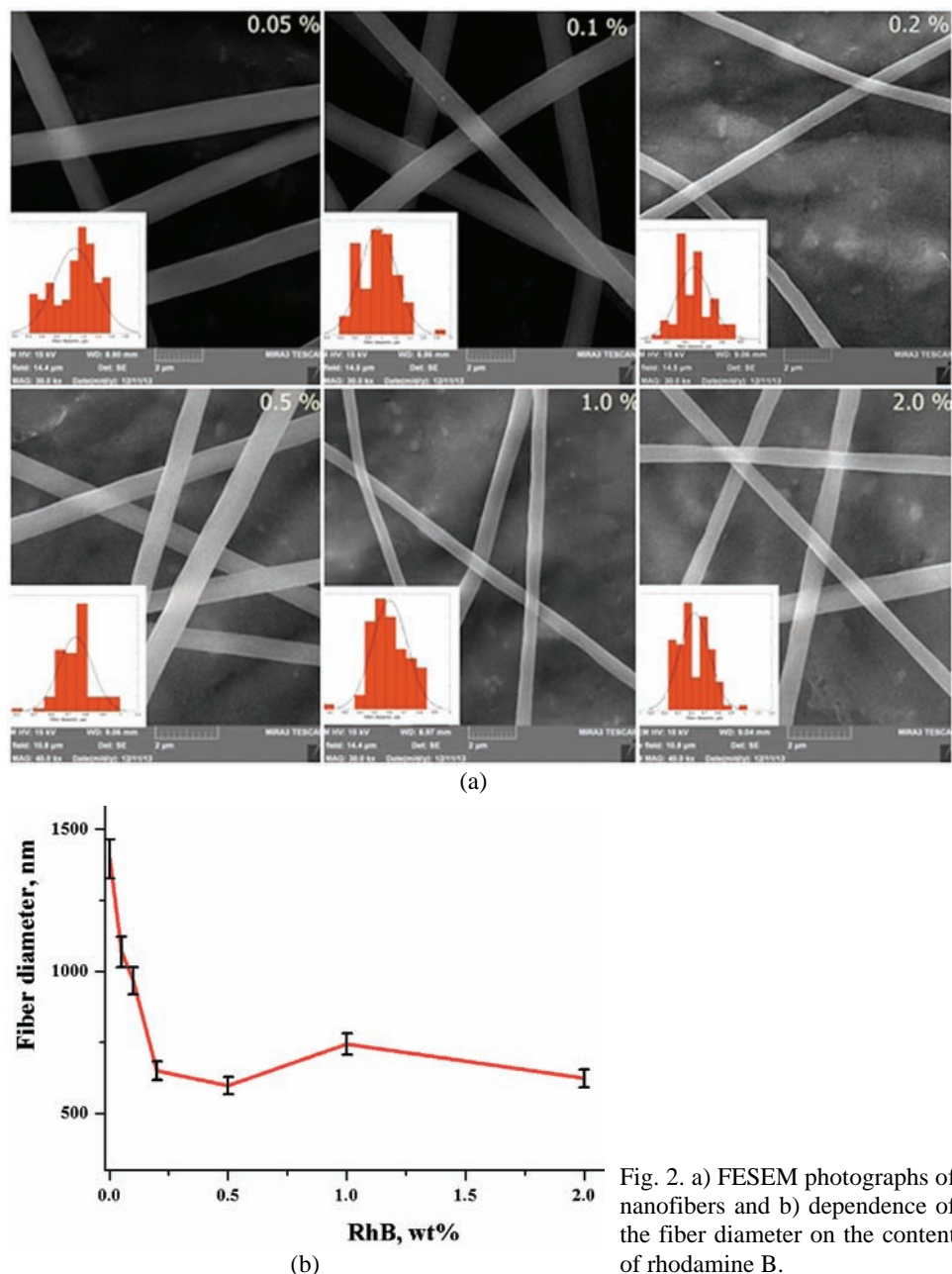


Fig. 2. a) FESEM photographs of nanofibers and b) dependence of the fiber diameter on the content of rhodamine B.

viour could be the change in the solution conductivity. RhB as a polar dye belongs to the xanthine family and it is easily dissolved in polar solvents, such as DMF. Depending on the pH of the solution, RhB can exists in a number of possible

molecular forms, such as cationic, zwitterionic, quinonic and lactonic.<sup>32</sup> Since ionic charges are in direct relation with the electrical conductivity of the solution, increasing the charge density on the surface of the ejected jet leads to an increase in the electric charges carried by the jet. When the conductivity of the solution is increased, more charges can be carried by the jet. An increase in the conductivity means that electrostatic forces can now overcome the surface tension more easily.<sup>34,35</sup> As a result, when the charge density increases in the jet, more stretching and elongation of the jet occurs during electrospinning, thereby causing a reduction in fiber diameter.

The fiber diameter decreased from  $1395 \pm 262$  nm for pure PMMA to  $598 \pm 115$  nm for PMMA doped with 1.0 wt. % RhB. The distribution of the fiber diameters followed the same trend, the standard deviation decreased from 362 nm for pure PMMA to 98 nm, and subsequently the concentration rose. These results indicated that for concentrations of RhB in the range 0.5–1.0 wt. %, the behavior of the solutions changed.

The FTIR spectra of pure poly (methyl methacrylate) (PMMA) fibers (spectrum a) and RhB (spectrum b) are presented in Fig. 3.

Fig. 3. FTIR spectra of a) poly(methyl methacrylate) fibers and b) RhB, and corresponding structural formulas of PMMA and RhB.

Available on line at [www.shd.org.rs/JSCS/](http://www.shd.org.rs/JSCS/)

(CC) 2014 SCS. All rights reserved.

Spectrum a exhibits vibrational bands typical for PMMA, *i.e.*, vibrational bands at 987 and 1453 cm<sup>-1</sup> that belong to O–CH<sub>3</sub> bending and stretching deformation of PMMA, respectively, bands at 1730 and 1250 cm<sup>-1</sup> that are assigned to stretching of C=O groups, a band at 1065 cm<sup>-1</sup> that could be ascribed to the C–O stretching vibration and a band at 1197 cm<sup>-1</sup> that belongs to the skeletal chain vibration. The other bands appearing in the 3000–2800 cm<sup>-1</sup>, 1490–1275 cm<sup>-1</sup> and 900–750 cm<sup>-1</sup> spectral regions correspond to different CH<sub>3</sub> and CH<sub>2</sub> vibrational modes.<sup>36,37</sup>

In spectrum b, vibrational bands corresponding to RhB can be seen. Namely, the broad intensity band at 3433 cm<sup>-1</sup> is associated with the O–H stretching vibration of hydroxyl groups. Its appearance is attributed to the absorption of water by the material. A weak intensity band at 3085 cm<sup>-1</sup> belongs to aromatic C–H vibrations, which also appear at 1130 cm<sup>-1</sup> (plane bending), 820 cm<sup>-1</sup> (out of plane bending) and at 685 cm<sup>-1</sup> (wagging vibrations). In addition, the band at 1710 cm<sup>-1</sup> belongs to the C=N stretching vibration, while the band at 1695 cm<sup>-1</sup> is associated with C=O stretching. A sharp absorption band appearing at 1590 cm<sup>-1</sup> was assigned to the asymmetric stretching vibration of the COO<sup>-</sup> group, the presence of which was further confirmed by the occurrence of a band at 1465 cm<sup>-1</sup>, ascribed to symmetric stretching of the group. The aromatic skeletal C–C stretch and C–O stretch could be observed at 1345 and 1250 cm<sup>-1</sup>, respectively.<sup>37,38</sup>

The FTIR spectra of PMMA fibers doped with different concentrations of the RhB, *i.e.*, 0.5, 1 and 2 wt. %, are presented in Fig. 4. The overall analysis of the spectra revealed that after the introduction of RhB into the PMMA fibers, the vibrational bands became more intense and their shape sharpened compared to

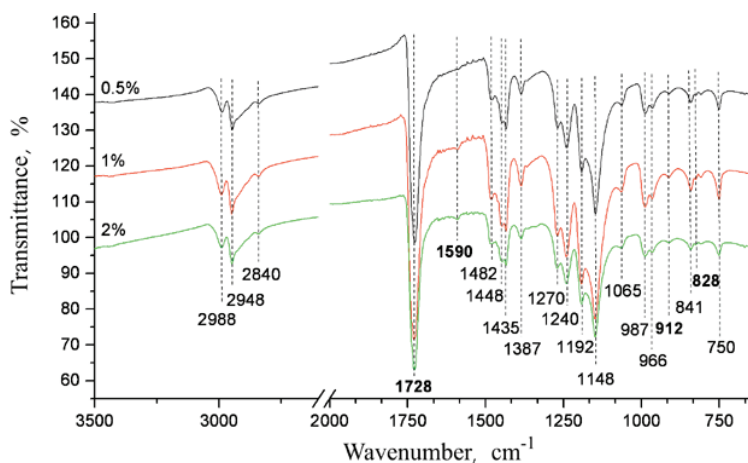


Fig. 4. FTIR spectra of poly(methyl methacrylate) fibers doped with different concentrations of RhB.

the corresponding bands of the pure PMMA fibers. Moreover, due to the presence of the RhB, the vibrational bands in the 3000–2800 cm<sup>-1</sup> and the 1750–1400 cm<sup>-1</sup> spectral regions were slightly shifted towards lower wavenumbers. Namely, these changes were the most visible in the case of the vibrational band at 1730, characteristic for the stretching of the C=O of PMMA fibers, which was strongly increased and insignificantly blue-shifted to the wavenumber 1728 cm<sup>-1</sup> after doping of the PMMA fibers with RhB. Since the band at 1695 cm<sup>-1</sup> associated with C=O stretching of the pure RhB (Fig. 3, spectrum b) does not appear in the spectra of PMMA doped with RhB (Fig. 4), the existence of such a strong band at 1728 cm<sup>-1</sup> could be attributed to the mutual vibrations of the C=O groups in the structure of PMMA fibers doped with RhB. In addition, the vibration of C=N groups of the RhB, found at 1710 cm<sup>-1</sup>, could also produce a slight shift in the band from 1730 to 1728 cm<sup>-1</sup>.

Detailed inspection of the IR spectra of PMMA fibers doped with RhB also revealed the formation of new vibrational bands of rather weak intensities, appearing at 1590, 912 and 828 cm<sup>-1</sup>. While the latter two could be attributed to the C–H vibration of the aromatic ring of RhB,<sup>35</sup> the appearance of the band at 1590 cm<sup>-1</sup>, characteristic for the COO<sup>-</sup> vibrations, confirms that RhB did not react with the functional groups of PMMA. By appearance of these peaks, the presence of RhB molecules within the PMMA matrix was confirmed, implying that the RhB was not chemically bonded but rather physically embedded within the PMMA matrix.<sup>18</sup>

The results of DSC analysis are given in the Fig. 5. The analyses were realized for pure powder PMMA, PMMA nanofibers and PMMA–RhB nanofibers of different compositions. The values of  $T_g$  and  $\Delta c_p/\Delta T$  are marked. The PMMA powder shows a  $T_g$  at 113.53 °C. It can be affirmed that the PMMA–solvent interaction was stronger, because the PMMA nanofibers electrospun from DMF solution had a  $T_g$  at 114.71 °C. The introduction of RhB into the polymer shifted the  $T_g$  to higher values up to a concentration of 0.5 wt. % (117.14 °C), but showed decreases at higher concentration. This is correlated to the viscosity/polarity-dependent behavior of RhB molecules in the solvent.<sup>39–41</sup> This is also in accord with the determined viscosity of the solutions with different concentrations of RhB. Having smaller dye–dye molecular distances, RhB in DMF permitted the formation of aggregates that were responsible for the reduction of the  $T_g$  of the fibers with higher contents of RhB.

A typical streak image of the fluorescence response of the fibers is shown in Fig. 6. The streak images acquired in gray scale are presented in pseudo-color, where different intensities are coded as different colors. The images were acquired in the photon counting mode operation; thus, the intensity corresponds to the number of counted photons. Wavelength scale (horizontal) is in the range between the 465 and 795 nm. Timescale (vertical) is about 50 ns. Laser excitation at 532

nm was also visible on the image. After deconvolution of the laser profile from the fluorescence response profile (green curve), an RhB fluorescence lifetime of about 3 ns was obtained, which is in agreement with published values.<sup>42,43</sup>

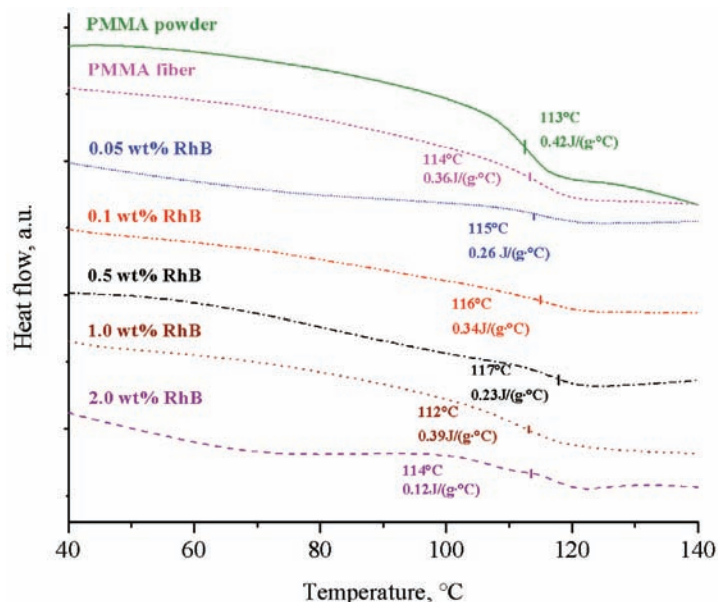


Fig. 5. DSC analysis of PMMA powder, PMMA nanofibers and PMMA-RhB nanofibers with different compositions.

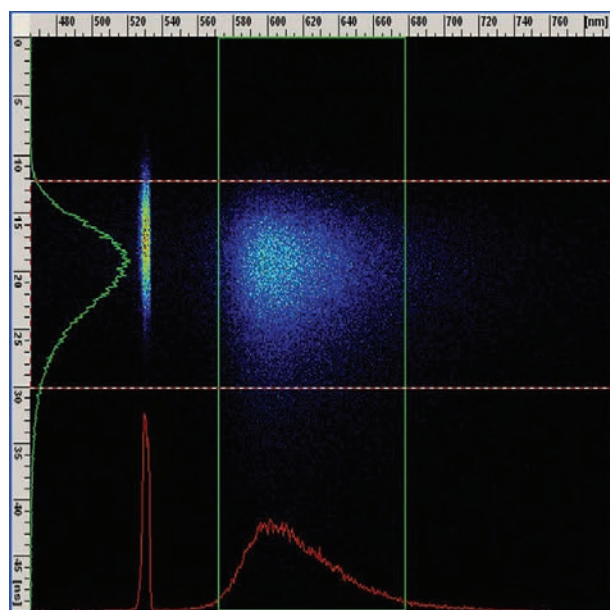


Fig. 6. A streak image of the fluorescence response of the PMMA-0.5 wt. % RhB fibers.

The fluorescence emission spectrum of the fibers is shown in Fig. 7. A shift of the fluorescence peak towards higher wavelengths could be noticed with increasing concentration of RhB. Increasing the concentration of the dye resulted in a red shift in the fluorescence wavelength as can be seen in Fig. 8, which shows the dependence of the wavelength of maximum emission on the concentration of RhB in PMMA. These results are in agreement with the literature.<sup>32,44</sup> It could also be noticed that a plateau was not reached.<sup>43</sup> When a plateau is reached, at high concentrations, aggregation formation restricts the peak shift.

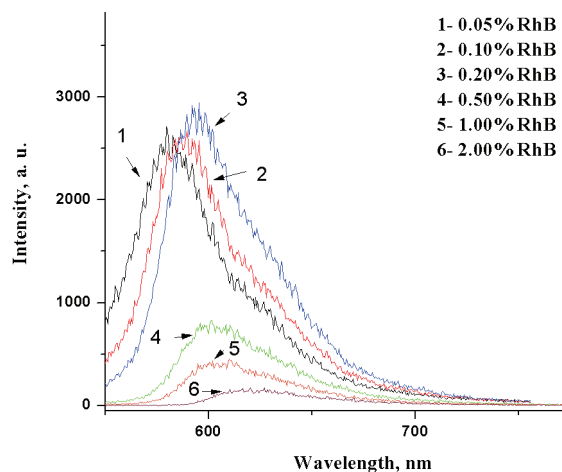


Fig. 7. Emission fluorescent spectrum of nanofibers with different contents of rhodamine B.

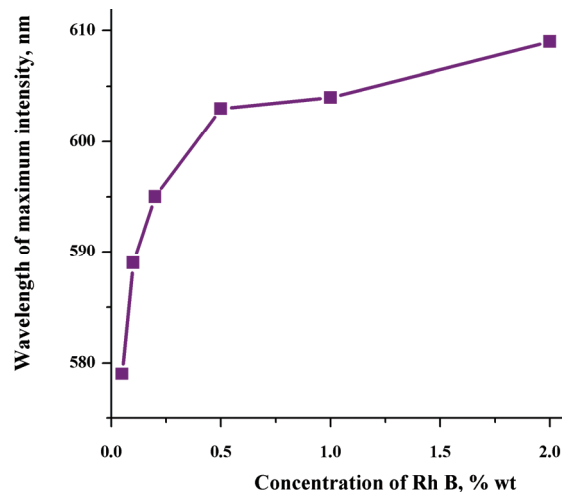


Fig. 8. Dependence of the wavelength of the maximum emission intensity on the content of rhodamine B.

The intensity of the fluorescence emission peak increased with concentration of RhB until 0.2 wt. % and then, at higher concentrations, it decreased and became broader, which is in agreement with published results for RhB in solution

and PMMA films.<sup>32,43</sup> This is correlated to the viscosity/polarity-dependent non-radioactive deactivation processes in RhB.

#### CONCLUSIONS

The electrospinning of PMMA doped with different contents of RhB was performed. Examination of the morphology of the formed fibers revealed bead-free nanofibers with a smooth surface and the mean diameter of the nanofibers decreased with increasing content of RhB in the PMMA. After addition of RhB into the PMMA, the  $T_g$  of the polymer increased with RhB content up to a concentration of 0.5 wt. %. The fluorescence response of fibers after laser excitation indicated that the emission peak increased with increasing concentration of RhB until 0.2 wt. %. The fluorescence emission intensity of RhB became broader and shifted to higher wavelength with increasing RhB concentration in the nanofibers. The values of the solution viscosity,  $T_g$  and fluorescence emission peak indicated that there was a significant and critical concentration of RhB (0.2–0.5 wt. %), and beyond these values the changes were in accord with their viscosity/polarity behavior.

*Acknowledgement.* This work was supported by the Ministry of Education, Science and Technology Development of the Republic of Serbia, Project Nos. TR 34011, III 45019 and 171020.

#### И З В О Д

#### ЕЛЕКТРОПРЕДЕЊЕ НАНОВЛАКАНА ПОЛИ(МЕТИЛМЕТАКРИЛАТА) ДОПИРАНОГ ЛАСЕРСКОМ БОЛОМ РОДАМИН Б

РАМДАН М. ДУКАЛИ<sup>1</sup>, ИВАНА М. РАДОВИЋ<sup>1</sup>, ДУШИЦА Б. СТОЈАНОВИЋ<sup>1</sup>, ДРАГУТИН М. ШЕВИЋ<sup>2</sup>,  
ВЕСНА Ј. РАДОЈЕВИЋ<sup>1</sup>, ДРАГАН М. ЈОЦИЋ<sup>1</sup> и РАДОСЛАВ Р. АЛЕКСИЋ<sup>1</sup>

<sup>1</sup>Универзитет у Београду, Технолошко-мештаришки факултет и <sup>2</sup>Универзитет у Београду,  
Институт за физику

У оквиру овог рада приказано је електропредење поли(метилметакрилат) допираниог родамина Б, које је веома перспективна техника за добијање фотолуминисцентних нановлакана. Изведен је процес електропредења нановлакана са различитим садржајем родамина Б од 0,05 до 2,0 мас. %. Интеракција полимерне матрице влакана и боје анализирана је применом методе Фуријеове трансформације инфрацрвеног спектра. Морфологија влакана као и величина и њихова расподела испитивана је помоћу SEM. Диференцијалном скенирајућом калориметријом анализирана су термичка својства, а оптичка својства техником ласерски индуковане флуоресценције (LIF). Добијена су влакна глатке површине и без мехурива. Анализа диференцијалном скенирајућом калориметријом је показала да  $T_g$  расте са порастом садржаја родамина Б у поли(метилметакрилату) до концентрације од 0,5 мас. %, а затим опада. При испитивању емисионог флуоресцентног спектра нановлакана, максимална флуоресцентна емисија је остварена при садржају родамина Б од 0,2 мас. %.

(Примљено 24. октобра 2013, ревидирано 27. јануара, прихваћено 30 јануара 2014)

## REFERENCES

1. Y. Xia, P. Yang, Y. Sun, Y. Wu, B. Mayers, B. Gates, Y. Yin, F. Kim, H. Yan, *Adv. Mater.* **5** (2003) 353
2. C. M. Lieber, *MRS Bull.* **287** (2003) 486
3. C. H. Wang, Y. Q. Dong, K. Sengothi, K. L. Tan, E. T. Kang, *Synth. Met.* **1021–1023** (1999) 1313
4. W. J. Li, C. T. Laurencin, E. J. Caterson, R. S. Tuan, F. K. Ko, *J. Biomed. Mater. Res.* **604** (2002) 613
5. X. Y. Wang, C. Drew, S. H. Lee, K. J. Senecal, J. Kumar, L. A. Samuelson, *Nano Lett.* **2** (2002) 1273
6. J. S. Kim, D. H. Reneker, *Polym. Compos.* **201** (1999) 124
7. S. Jiang, G. Duan, H. Hou, A. Greiner, S. Agarwal, *ACS Appl. Mater. Interfaces* **4** (2012) 4366
8. N. Tomczak, S. Gu, M. Han, N. F. van Hulst, G. J. Vancso, *Eur. Polym. J.* **42** (2006) 2205
9. Y. Shen, P. N. Prasad, *Appl. Phys., B* **74** (2002) 641
10. H. Q. Yu, B. J. Li, *Sci. Rep.* **3** (2013) 1674
11. R. Dersch, M. Steinhart, U. Boudriot, A. Greiner, J. H. Wendorff, *Polym. Adv. Technol.* **16** (2005) 276
12. K. J. Lee, J. H. Ho, Y. Kim, J. Jang, *Adv. Mater.* **18** (2006) 2216
13. A. Noy, A. E. Miller, J. E. Klare, B. L. Weeks, B. W. Woods, J. J. De Yoreo, *Nano Lett.* **2** (2002) 109
14. F. Quochi, F. Cordella, A. Mura, G. Dongiovanni, F. Balzer, H.-G. Rubahn, *Appl. Phys. Lett.* **88** (2006) 041106
15. H. Yu, Baojun Li, *Sci. Rep.* **3** (2013) 1674
16. D. Pisignano, G. Maruccio, E. Mele, L. Persano, F. Di Benedetto, R. Cingolani, *Appl. Phys. Lett.* **87** (2005) 123109
17. A. Formhals, US Patent 2,116,942 (1938)
18. C. Y. Hsu, Y. L. Liu, *J. Colloid Interface Sci.* **350** (2010) 75
19. A. G. Kanani, S. H. Bahrami, *Trends Biomater. Artif. Organs* **24** (2010) 93
20. D. H. Reneker, I. Chun, *Nanotechnology* **7** (1996) 216
21. R. Jaeger, H. Schonherr, G. J. Vancso, *Macromolecules* **29** (1996) 7634
22. M. Bognitzki, W. Czado, T. Frese, A. Schaper, M. Hellwig, M. Steinhart, *Adv. Mater.* **13** (2001) 70
23. S. Schlecht, S. Tan, M. Yosef, R. Dersch, J. H. Wendorff, Z. Jia, A. Schaper, *Chem. Mater.* **17** (2005) 809
24. X. Wang, S.-H. Lee, B.-C. Ku, L. A. Samuelson, J. Kumar, *J. Macromol. Sci., A* **39** (2002) 1241
25. J. L. Davis, K. Guzan, K. Mills, L. Han, in *Proceedings of NSTI-Nanotech 2010*, Nanotechnology Anaheim, CA, USA, 2010, p. 769
26. A. Tagaya, Y. Koike, T. Kinoshita, E. Nihei, T. Yamamoto, K. Sasaki, *Appl. Phys. Lett.* **63** (1993) 883
27. G. Somasundaran, A. Ramalingam, *Opt. Laser Technol.* **31** (1999) 351
28. H. Liang, Z. Zheng, Z. Li, J. Xu, B. Chen, H. Zhao, Q. Zhang, H. Ming, *J. Appl. Polym. Sci.* **93** (2004) 681
29. K. Geetha, M. Rajesh, V. P. N. Nampoori, C. P. G. Vallabhan, P. Radhakrishnan, *J. Opt., A* **6** (2004) 379
30. P. Kumar, D. R. Bajpai, M. Keller, *Microsyst. Technol.* **14** (2008) 1165

31. G. Sreekumar, P. G. Louie Fobel, S. Sreeja, S. R. Suresh, S. Mayadevi, C. I. Muneera, C. S. Suchand Sandeep, R. Philip, C. Mukharjee, *Chem. Phys. Lett.* **506** (2011) 61
32. M. Fikry, M. M. Omar, L. Z. Ismail, *J. Fluoresc.* **19** (2009) 741
33. H. Wang, Q. Liu, Q. Yang, Y. Li, W. Wang, L. Sun, C. Zhang, Y. Li, *J. Mater. Sci.* **45** (2010) 1032
34. C. Hsu, S. Shivkumar, *Macromol. Mater. Eng.* **289** (2004) 334
35. T. Jarusuwannapoom, W. Hongrojjanawiwat, S. Jitjaicham, L. Wannatong, M. Nithitanakul, C. Pattamaprom, P. Koombhongse, R. Rangkupan, P. Supaphol, *Eur. Polym. J.* **41** (2005) 409
36. I. S. Elashmawi, N. A. Hakeem, *Polym. Eng. Sci.* **48** (2008) 895
37. G. Socrates, *Infrared and Raman Characteristic Group Frequencies*, Wiley, New York, 2001, p. 347
38. A. A. M. Farag, I. S. Yahia, *Opt. Commun.* **283** (2010) 4310
39. A. V. Deshpande, E. B. Namdas, *J. Lumin.* **91** (2000) 25
40. N. Patra, A. C. Barone, M. Salerno, *Adv. Polym. Tech.* **30** (2011) 12
41. S. S. Musbah, V. Radojević, I. Radović, P. S. Uskoković, D. B. Stojanović, M. Dramićanin, R. Aleksić, *J. Min. Metall., B* **48** (2012) 309
42. T. W. J. Gadella, Jr., T. M. Jovin, R. M. Clegg, *Biophys. Chem.* **48** (1993) 2219
43. T. Robinson, Y. Schaerli, R. Wootton, F. Hollfelder, C. Dunsby, G. Baldwin, M. Neil, P. French, A. de Mello, *Lab Chip* **9** (2009) 3437
44. M. F. Al-Kadhemy, I. F. Alsharuee, A. D. Al-Zuky, *J. Phys. Sci.* **22** (2011) 77.